

 Open access • Journal Article • DOI:10.1103/PHYSREVD.89.114004

## Probing new physics in diphoton production with proton tagging at the Large Hadron Collider — Source link

Sylvain Fichet, G. von Gersdorff, Oldrich Kepka, Bruno Lenzi ...+2 more authors

**Institutions:** International Institute of Minnesota, Spanish National Research Council, Academy of Sciences of the Czech Republic, CERN

**Published on:** 03 Jun 2014 - Physical Review D (American Physical Society)

Related papers:

- [Anomalous quartic  \$WW\gamma\gamma\$ ,  \$ZZ\gamma\gamma\$ , and trilinear  \$WW\gamma\$  couplings in two-photon processes at high luminosity at the LHC](#)
- [Anomalous  \$WW\gamma\$  coupling in photon-induced processes using forward detectors at the CERN LHC](#)
- [The Two photon particle production mechanism. Physical problems. Applications. Equivalent photon approximation](#)
- [Light-by-light scattering with intact protons at the LHC: from standard model to new physics](#)
- [Probing quartic neutral gauge boson couplings using diffractive photon fusion at the LHC](#)

Share this paper:    

View more about this paper here: <https://typeset.io/papers/probing-new-physics-in-diphoton-production-with-proton-1bkmr08pm3>

# Probing new physics in diphoton production with proton tagging at the Large Hadron Collider

S. Fichtel,<sup>1,\*</sup> G. von Gersdorff,<sup>2,†</sup> O. Kepka,<sup>3,‡</sup> B. Lenzi,<sup>4,§</sup> C. Royon,<sup>5,¶</sup> and M. Saimpert<sup>5,\*\*</sup>

<sup>1</sup>*International Institute of Physics, UFRN, Avenida Odilon Gomes de Lima, 1722, Capim Macio, 59078-400 Natal, RN, Brazil*

<sup>2</sup>*ICTP SAIFR, Instituto de Fisica Teorica, Sao Paulo State University, Sao Paulo 01140-070, Brazil*

<sup>3</sup>*Institute of Physics of the Academy of Sciences, 18221 Prague 8, Czech Republic*

<sup>4</sup>*CERN, CH-1211 Geneva 23, Switzerland*

<sup>5</sup>*IRFU/Service de Physique des Particules, CEA/Saclay, 91191 Gif-sur-Yvette cedex, France*

(Received 18 December 2013; published 3 June 2014)

The sensitivities to anomalous quartic photon couplings at the Large Hadron Collider are estimated using diphoton production via photon fusion. The tagging of the protons proves to be a very powerful tool to suppress the background and unprecedented sensitivities down to  $7 \times 10^{-15} \text{ GeV}^{-4}$  are obtained, providing a new window on extra dimensions and strongly interacting composite states in the multi-TeV range. Generic contributions to quartic photon couplings from charged and neutral particles with arbitrary spin are also presented.

DOI: 10.1103/PhysRevD.89.114004

PACS numbers: 13.85.Qk, 12.20.Fv, 12.60.Cn, 14.70.Bh

Several major experimental and conceptual facts, like the overwhelming evidence for dark matter or the gauge-hierarchy problem, point towards the existence of new physics beyond the Standard Model (SM) at a scale relatively close to the electroweak scale. In spite of naturalness arguments, this paradigm of a TeV-scale new physics is challenged by both direct searches at the Large Hadron Collider (LHC) and by indirect measurements like the Large Electron Positron (LEP) electroweak precision tests. In the scenario of new physics out of reach from direct observation at the LHC, one may expect that the first manifestations show up in precision measurements of the SM properties. Such powerful precision tests are already well advanced in the electroweak and flavor sectors of the SM, and distortions of the newly discovered Higgs sector are also being scrutinized. However, another sector of the SM can be tested with high precision at the LHC, the one of pure gauge interactions.

In this article, four-photon ( $4\gamma$ ) interactions through diphoton production via photon fusion with intact outgoing protons are considered (Fig. 1). Interactions between photons and  $Z$ ,  $W$  bosons in a similar case have already been studied [1]. The only existing direct limits on  $4\gamma$  interactions originate from low energy laser experiments [2]. The study of this process in LHC proton-proton collisions at center-of-mass energy of  $\sqrt{s} = 14 \text{ TeV}$  will benefit from the new forward proton detectors considered in the ATLAS and CMS/TOTEM experiments [3]. We first provide the generic

new physics contributions to the  $4\gamma$  couplings and point out sizable contributions from strongly coupled and warped-extra dimension scenarios. The sensitivities of the upgrades of the ATLAS and CMS/TOTEM experiments are then given including all backgrounds.

In the assumption of a new physics mass scale  $\Lambda$  heavier than experimentally accessible energy  $E$ , all new physics manifestations can be described using an effective Lagrangian valid for  $\Lambda \gg E$ . Among these operators, the pure photon dimension-eight operators

$$\mathcal{L}_{4\gamma} = \zeta_1^\gamma F_{\mu\nu} F^{\mu\nu} F_{\rho\sigma} F^{\rho\sigma} + \zeta_2^\gamma F_{\mu\nu} F^{\nu\rho} F_{\rho\lambda} F^{\lambda\mu} \quad (1)$$

can induce the  $\gamma\gamma \rightarrow \gamma\gamma$  process, highly suppressed in the SM [4,5]. We discuss here possible new physics contributions to  $\zeta_{1,2}^\gamma$  that can be probed and discovered at the LHC using the forward proton detectors. For the first time, we provide the complete list of contributions to  $\zeta_{1,2}$  from particles with arbitrary quantum numbers, at both tree and loop level. This parametrization is useful for the study of a broad class of models. We also derive the predictions from present models, finding large contributions from warped Kaluza Klein (KK) gravitons [6] and from the strongly interacting radion/dilaton [7].

Loops of heavy charged particles contribute to the  $4\gamma$  couplings [4] as  $\zeta_i^\gamma = \alpha_{\text{em}}^2 Q^4 m^{-4} N c_{i,s}$ , where

$$c_{1,s} = \begin{cases} \frac{1}{288} & s = 0 \\ -\frac{1}{36} & s = \frac{1}{2} \\ -\frac{5}{32} & s = 1 \end{cases}, \quad c_{2,s} = \begin{cases} \frac{1}{360} & s = 0 \\ \frac{7}{90} & s = \frac{1}{2} \\ \frac{27}{40} & s = 1 \end{cases} \quad (2)$$

where  $s$  denotes the spin of the heavy particle of mass  $m$  running in the loop and  $Q$  its electric charge. The factor  $N$

\*sylvain.fichtel@lpsc.in2p3.fr

†gersdorff@gmail.com

‡kepka@fzu.cz

§bruno.lenzi@cern.ch

¶christophe.royon@cea.fr

\*\*matthias.saimpert@cern.ch

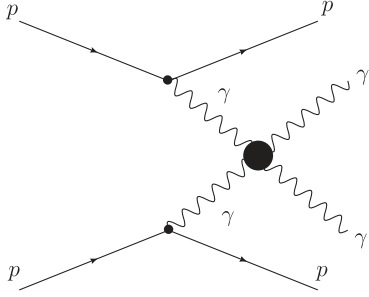


FIG. 1. Diphoton production via photon fusion sensitive to  $4\gamma$  anomalous couplings. Both protons are intact in the final state.

counts all additional multiplicities such as color or flavor. These couplings scale as  $\sim Q^4$  and are enhanced in presence of particles with large charges. For example, certain light composite fermions, characteristic of composite Higgs models, have typically electric charges of several units [4]. For a 500 GeV vector (fermion) resonance with  $Q = 3(4)$ , large couplings  $\zeta_i^\gamma$  of the order of  $10^{-13} - 10^{-14}$  GeV $^{-4}$  can be reached.

Beyond perturbative contributions to  $\zeta_i^\gamma$  from charged particles, nonrenormalizable interactions of neutral particles are also present in common extensions of the SM. Such theories can contain scalar, pseudoscalar and spin-2 resonances, respectively denoted  $\varphi$ ,  $\tilde{\varphi}$ ,  $h^{\mu\nu}$ , that couple to the photon as

$$\mathcal{L}_{\gamma\gamma} = f_{0^+}^{-1} \varphi (F_{\mu\nu})^2 + f_{0^-}^{-1} \tilde{\varphi} F_{\mu\nu} F_{\rho\lambda} \epsilon^{\mu\nu\rho\lambda} + f_2^{-1} h^{\mu\nu} (-F_{\mu\rho} F_{\nu}^{\rho} + \eta_{\mu\nu} (F_{\rho\lambda})^2 / 4), \quad (3)$$

and generate the  $4\gamma$  couplings by tree-level exchange as  $\zeta_{i,s}^\gamma = (f_{i,s} m)^{-2} d_{i,s}$ , where

$$d_{1,s} = \begin{cases} \frac{1}{2} & s = 0^+ \\ -4 & s = 0^- \\ -\frac{1}{8} & s = 2 \end{cases}, \quad d_{2,s} = \begin{cases} 0 & s = 0^+ \\ 8 & s = 0^- \\ \frac{1}{2} & s = 2 \end{cases}. \quad (4)$$

Strongly coupled conformal extensions of the SM contain a scalar particle ( $s = 0^+$ ), the dilaton. In the case of small explicit conformal breaking, the dilaton is light and couples only weakly to the photon,  $f_\varphi^{-1} \ll m_\varphi^{-1}$ . However, a more natural situation occurs when explicit conformal breaking is large [7–9], in which case the dilaton has a mass comparable to the other resonances of the theory and can be much more strongly coupled  $f_\varphi^{-1} \sim \pi/m_\varphi$ , as long as photons are mostly composite. In this case, even a 2 TeV dilaton can produce a sizable effective photon interaction,  $\zeta_1^\gamma \sim 10^{-13}$  GeV $^{-4}$ .

These features are reproduced at large number of colors by the gauge-gravity correspondence in a warped-extra dimension. The dilaton is identified as the radion, and a mainly composite photon corresponds to a large infrared

(IR) brane kinetic term. Warped-extra dimensions also feature KK gravitons [6]. These are interpreted as spin-2 resonances in the gauge theory. A mostly elementary photon does not yield a sizeable coupling. However, a mostly composite one couples more strongly to the KK fields, in that case the whole set of KK modes induces [4]

$$\zeta_i^\gamma = \frac{\kappa^2}{8\tilde{k}^4} d_{i,2}, \quad (5)$$

where  $\tilde{k}$  is the IR scale that determines the first KK graviton mass as  $m_2 = 3.83\tilde{k}$ , and  $\kappa$  is a parameter that can be taken  $O(1)$ . For  $\kappa \sim 1$ , and  $m_2 \lesssim 6$  TeV, the photon vertex can easily exceed  $\zeta_2^\gamma \sim 10^{-14}$  GeV $^{-4}$ .

Present searches for warped-extra dimensions at the LHC in the diphoton channel have been mainly performed in looking for resonances in the diphoton mass spectrum, which leads to the best present limits at low  $\kappa$  [10]. At high  $\kappa$ , the narrow-width approximation for warped KK gravitons breaks down, such that the excess is more difficult to detect. In contrast, this is precisely in the high- $\kappa$  regime that the warped-extra dimension searches through  $4\gamma$  vertices are the more competitive, as the effective operators are valid for arbitrary large  $\kappa$ . Both type of searches are therefore complementary.

Since we deal with nonrenormalizable couplings perturbative unitarity (and effective field theory) breaks down at some scale  $\Lambda'$ . This can partially be avoided by using full amplitudes, but even then some couplings (such as the dilaton coupling  $f_\varphi^{-1}$ ) grow with energy. Whenever the scale  $\Lambda'$  falls below the detector acceptance a form factor  $1/(1 + (m_{\gamma\gamma}/\Lambda')^4)$  is applied to mimic the effects that restore unitarity [5]. However, for completeness sensitivities with  $\Lambda' = 1$  TeV are quoted. The form factor is only required for light new physics states of mass  $\leq 2$  TeV (1 TeV) for states contributing at tree level (loop level). For heavier masses the experimentally achievable center-of-mass energies lie below the one for single (pair) production of the new particles, and effective field theory is valid. In many cases such a form factor is not necessary (for instance, when the new particles have a large enough mass).

The  $\gamma\gamma \rightarrow \gamma\gamma$  process (Fig. 1) can be probed via the detection of two intact protons in the forward proton detectors proposed by the ATLAS and CMS [3] Collaborations, and two energetic photons in the corresponding electromagnetic calorimeters [11,12]. The forward detectors are expected to be located symmetrically at about 210 m from the main interaction point and cover the range  $0.015 < \xi < 0.15$ , where  $\xi$  is the fractional proton momentum loss. The time of flight of the scattered proton can be measured with a precision of  $\sim 10$  ps that allows us to determine the production point of the protons within 2.1 mm inside ATLAS/CMS and to check if they originate from the same scattering vertex as the two photons. It is worth noticing that the SM cross section of diphoton production

TABLE I. Number of signal (for  $\zeta_1 = 2 \times 10^{-13} \text{ GeV}^{-4}$ ) and background events after various selections for an integrated luminosity of  $300 \text{ fb}^{-1}$  and  $\mu = 50$  at  $\sqrt{s} = 14 \text{ TeV}$ . At least one converted photon is required. Excl. stands for exclusive backgrounds and DPE for double pomeron exchange backgrounds (see text).

Cut/process	Signal	Excl.	DPE	$e^+e^-$ , dijet + pileup	$\gamma\gamma$ + pileup
$0.015 < \xi < 0.15$ , $p_{T1,2} > 50 \text{ GeV}$	20.8	3.7	48.2	$2.8 \times 10^4$	$1.0 \times 10^5$
$p_{T1} > 200 \text{ GeV}$ , $p_{T2} > 100 \text{ GeV}$	17.6	0.2	0.2	1.6	2968
$m_{\gamma\gamma} > 600 \text{ GeV}$	16.6	0.1	0	0.2	1023
$p_{T2}/p_{T1} > 0.95$ , $ \Delta\phi  > \pi - 0.01$	16.2	0.1	0	0	80.2
$\sqrt{\xi_1 \xi_2 s} = m_{\gamma\gamma} \pm 3\%$	15.7	0.1	0	0	2.8
$ y_{\gamma\gamma} - y_{pp}  < 0.03$	15.1	0.1	0	0	0

with intact protons is dominated by the QED process at high diphoton mass—and not by gluon exchanges—and is thus very well known. If the protons are not intact, the two-photon quasielastic diphoton production with large theoretical uncertainties needs to be considered [13], leading to a large uncertainty in the background determination. In the present case, any deviation from the standard model prediction will be a sign of beyond SM effects.

The electromagnetic calorimeters cover the pseudorapidity range  $|\eta| \lesssim 2.5$  and provide excellent resolution in terms of energy ( $< 1\%$  at transverse momenta  $p_T > 100 \text{ GeV}$ ) and position (0.001 in  $\eta$  and 1 mrad in the azimuthal angle  $\phi$ ) for photons with  $p_T$  ranging from few GeV to few TeV [14]. A fraction of the photons ( $\sim 15\%$ – $30\%$ ) converts to electron-positron pairs in the region instrumented with silicon tracking detectors. The reconstruction of at least one conversion allows us to locate the photon production point with submillimeter accuracy and, when combined with the information from the proton detectors, constrains the full event kinematics. This is extremely powerful to reject backgrounds with real or fake photons from a hard scattering process and protons coming from additional interactions occurring in the same or neighboring bunch crossings (pileup). The average number of multiple proton-proton collisions per bunch crossing is denoted as  $\mu$  in the following. In the case of the ATLAS detector, the production point of the photons can be determined within  $\sim 15 \text{ mm}$  exploiting the longitudinal segmentation of the ATLAS calorimeter [15]. Consequently, an alternative scenario with no converted photons is also considered.

According to Ref. [16], even in the presence of more than 100 pileup interactions, the photon identification efficiency is expected to be around 75% for  $p_T > 100 \text{ GeV}$ , with jet rejection factors exceeding 4000. In addition, about 1% of the electrons are misidentified as photons. These numbers are used in the phenomenological study presented below.

The anomalous  $\gamma\gamma \rightarrow \gamma\gamma$  process has been implemented in the Forward Physics Monte Carlo (FPMC) generator [17] that aims at providing a variety of diffractive and photon-induced processes in a common framework, including a survival probability of 0.9. This factor is necessary to take into account the possibility of additional soft interactions occurring between the two intact protons.

The FPMC generator was used to simulate the signal and background processes giving rise to two intact protons accompanied by two photons, electrons or jets that can mimic the photon signal. Those include exclusive SM production of  $\gamma\gamma \rightarrow \gamma\gamma$  via lepton and quark boxes and  $\gamma\gamma \rightarrow e^+e^-$ . The central exclusive production of  $\gamma\gamma$  via two-gluon exchange, not present in FPMC, was simulated using ExHuME [18]. This series of backgrounds is called “Exclusive” in Table I and Figs. 2, 3. FPMC was also used to produce  $\gamma\gamma$ , Higgs to  $\gamma\gamma$  and dijet productions via double pomeron exchange (called DPE background in Table I and Fig. 2). Such backgrounds tend to be softer than the signal and can be suppressed with requirements on the transverse momenta of the photons ( $p_{T1} > 200 \text{ GeV}$  for the leading and  $p_{T2} > 100 \text{ GeV}$  for the subleading photons, respectively) and the diphoton invariant mass ( $m_{\gamma\gamma} > 600 \text{ GeV}$ ), as shown in Fig. 2. The shape of the signal distribution is similar for  $\zeta_2$  with a different normalization. In addition, the final-state photons of the signal are typically back to back and have about the same transverse momenta. Requiring a large azimuthal angle  $|\Delta\phi| > \pi - 0.01$  between the two photons and a ratio  $p_{T2}/p_{T1} > 0.95$  greatly reduces the contribution of non-exclusive processes.

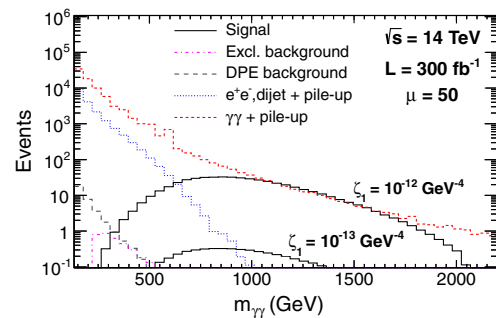


FIG. 2 (color online). Diphoton invariant mass distribution for the signal [ $\zeta_1 = 10^{-12}, 10^{-13} \text{ GeV}^{-4}$ , see Eq. (1)] and for the backgrounds (dominated by  $\gamma\gamma$  with protons from pileup), requesting two protons in the forward detectors and two photons of  $p_T > 50 \text{ GeV}$  with at least one converted photon in the central detector, for a luminosity of  $300 \text{ fb}^{-1}$  and an average pileup of  $\mu = 50$ . Excl. stands for exclusive backgrounds and DPE for double pomeron exchange backgrounds (see text).

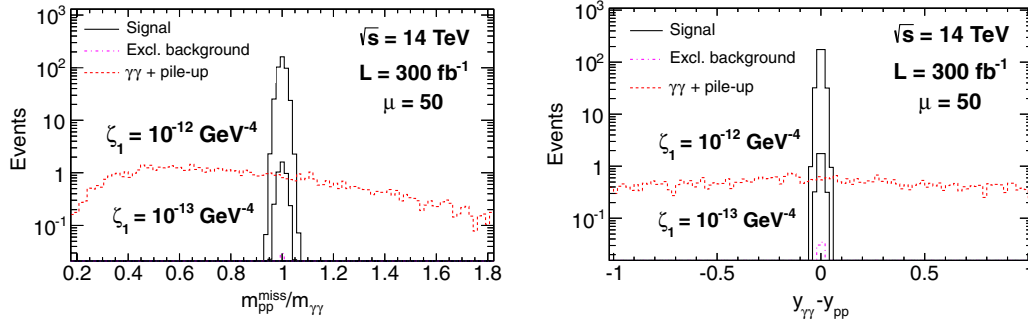


FIG. 3 (color online). Diphoton to missing proton mass ratio (left) and rapidity difference (right) distributions for signal considering two different coupling values [ $10^{-12}$  and  $10^{-13}$   $\text{GeV}^{-4}$ , see Eq. (1)] and for backgrounds after requirements on photon  $p_T$ , diphoton invariant mass,  $p_T$  ratio between the two photons and on the angle between the two photons. At least one converted photon is required. The integrated luminosity is  $300 \text{ fb}^{-1}$  and the average pileup is  $\mu = 50$ .

Additional background processes include the quark and gluon-initiated production of two photons, two jets and Drell-Yan processes leading to two electrons. The two intact protons arise from pileup interactions (these backgrounds are called  $\gamma\gamma + \text{pileup}$  and  $e^+e^-$ , dijet + pileup in Table I). The hard scattering processes are simulated with the HERWIG 6.5 [19] generator while the pileup interactions are simulated by PYTHIA8 [20]. The probability to detect at least one proton in each of the two forward detectors is estimated to be 32%, 66% and 93% for 50, 100 and 200 additional interactions, respectively. The pileup background is further suppressed by requiring the proton missing invariant mass to match the diphoton invariant mass within the expected resolution ( $m_{pp}^{\text{miss}} = \sqrt{\xi_1 \xi_2 s} = m_{\gamma\gamma} \pm 3\%$ ), and the diphoton system rapidity and the rapidity of the two protons defined as  $y_{pp} = 0.5 \ln(\frac{\xi_1}{\xi_2})$  to be the same within the resolution ( $|y_{\gamma\gamma} - y_{pp}| < 0.03$ ), as shown in Fig. 3.

The number of expected signal and background events passing respective selections is shown in Table I for an integrated luminosity of  $300 \text{ fb}^{-1}$  ( $\approx 3$  years of data taking at the LHC) and 50 pileup interactions for a center-of-mass energy of 14 TeV. It is required that at least one photon converts in the tracker. Gaussian smearings of 1% for the total energy, 0.001 for the pseudorapidity and 1 mrad for the azimuthal angle are applied to each photon. Exploiting the full event kinematics with the forward proton detectors allows us to completely suppress the background with a signal selection efficiency after the acceptance cuts exceeding 70%. Tagging the protons is absolutely needed to suppress the  $\gamma\gamma + \text{pileup}$  events. Further background reduction is even possible by requiring the photons and the protons to originate from the same vertex that provides an additional rejection factor of 40 for 50 pileup interactions, showing the large margin on the background suppression. A similar study at a higher pileup of 200 was performed and led to a negligible background (0.3 expected background events for  $300 \text{ fb}^{-1}$ ), showing the robustness of this analysis. Moreover, if one relaxes the request of at least one photon to be converted, the signal is increased by a factor 3 to 4. The

sensitivities on photon quartic anomalous couplings are given in Table II for different scenarios corresponding to the medium luminosity at the LHC ( $300 \text{ fb}^{-1}$ ) and the high luminosity ( $3000 \text{ fb}^{-1}$  in ATLAS) with and without form factor. The sensitivity extends up to  $7 \times 10^{-15} \text{ GeV}^{-4}$  allowing us to probe further the models of new physics described above. Using a form factor with higher values of  $\Lambda' = 2 \text{ TeV}$  leads to similar results as without form factors.

In this article, the sensitivities to quartic photon couplings at the LHC, obtained by measuring the photons in the central CMS and ATLAS detectors and the intact protons in dedicated forward proton detectors, are estimated. For the first time, sensitivities on anomalous quartic couplings are large enough to probe models of new physics. The imprint of warped KK gravitons and of a strongly coupled dilaton can be discovered in the multi-TeV range. Also, a generic 500 GeV fermion (vector) resonance can be probed for electric charge  $Q \gtrsim 4$  (3) via loop effects. The analysis greatly benefits from the kinematical constraints from the photon and proton measurements, which allows us to obtain negligible backgrounds.

TABLE II.  $5\sigma$  discovery and 95% C.L. exclusion limits on  $\zeta_1$  and  $\zeta_2$  couplings in  $\text{GeV}^{-4}$  [see Eq. (1)] with and without form factor (f.f.) with  $\Lambda' = 1 \text{ TeV}$ , requesting at least one converted photon ( $\geq 1 \text{ conv } \gamma$ ) or not (all  $\gamma$ ). All sensitivities are given for  $300 \text{ fb}^{-1}$  and  $\mu = 50$  pileup events (medium luminosity LHC) except for the numbers of the last column which are given for  $3000 \text{ fb}^{-1}$  and  $\mu = 200$  pileup events (high luminosity LHC) where we do not request converted photons in the case of ATLAS.

Luminosity	$300 \text{ fb}^{-1}$	$300 \text{ fb}^{-1}$	$300 \text{ fb}^{-1}$	$3000 \text{ fb}^{-1}$
Pileup ( $\mu$ )	50	50	50	200
Coupling ( $\text{GeV}^{-4}$ )	$\geq 1 \text{ conv } \gamma$	$\geq 1 \text{ conv } \gamma$	all $\gamma$	all $\gamma$
	$5\sigma$	95% C.L.	95% C.L.	95% C.L.
$\zeta_1$ f.f.	$1. \times 10^{-13}$	$9. \times 10^{-14}$	$5. \times 10^{-14}$	$2.5 \times 10^{-14}$
$\zeta_1$ no f.f.	$3.5 \times 10^{-14}$	$2.5 \times 10^{-14}$	$1.5 \times 10^{-14}$	$7. \times 10^{-15}$
$\zeta_2$ f.f.	$2.5 \times 10^{-13}$	$1.5 \times 10^{-13}$	$1. \times 10^{-13}$	$4.5 \times 10^{-14}$
$\zeta_2$ no f.f.	$7.5 \times 10^{-14}$	$5.5 \times 10^{-14}$	$3. \times 10^{-14}$	$1.5 \times 10^{-14}$

## ACKNOWLEDGMENTS

We thank useful discussions with Christophe Grojean.

- 
- [1] E. Chapon, O. Kepka, and C. Royon, *Phys. Rev. D* **81**, 074003 (2010); O. Kepka and C. Royon, *Phys. Rev. D* **78**, 073005 (2008); J. de Favereau *et al.*, arXiv:0908.2020.
- [2] M. Bregant *et al.*, *Phys. Rev. D* **78**, 032006 (2008).
- [3] ATLAS Collaboration, Report No. CERN-LHCC-2011-012; TOTEM Collaboration, Report No. CERN-LHCC-2013-009.
- [4] S. Fichet and G. von Gersdorff, *J. High Energy Phys.* **03** (2014) 102.
- [5] R. S. Gupta, *Phys. Rev. D* **85**, 014006 (2012).
- [6] L. Randall and R. Sundrum, *Phys. Rev. Lett.* **83**, 3370 (1999).
- [7] Z. Chacko, R. K. Mishra and D. Stolarski, *J. High Energy Phys.* **09** (2013) 121.
- [8] Z. Chacko and R. K. Mishra, *Phys. Rev. D* **87**, 115006 (2013).
- [9] B. Bellazzini, C. Csáki, J. Hubisz, J. Serra, and J. Terning, *Eur. Phys. J. C* **73**, 2333 (2013).
- [10] ATLAS Collaboration, *New J. Phys.* **15**, 043007 (2013).
- [11] ATLAS Collaboration, *JINST* **3**, S08003 (2008).
- [12] CMS Collaboration, *JINST* **3**, S08004 (2008).
- [13] M. Luszczak and A. Szczurek, arXiv:1309.7201.
- [14] ATLAS Collaboration, Report No. CERN-OPEN-2008-020, <http://cdsweb.cern.ch/record/1125884>.
- [15] ATLAS Collaboration, *Phys. Lett. B* **716**, 1 (2012).
- [16] ATLAS Collaboration, Report No. ATL-PHYS-PUB-2013-009.
- [17] M. Boonekamp *et al.*, arXiv:1102.2531.
- [18] J. Monk and A. Pilkington, *Comput. Phys. Commun.* **175**, 232 (2006); V. A. Khoze, A. D. Martin, and M. G. Ryskin, *Eur. Phys. J. C* **55**, 363 (2008).
- [19] G. Corcella *et al.*, arXiv:hep-ph/0210213.
- [20] T. Sjostrand, S. Mrenna, and P. Z. Skands, *Comput. Phys. Commun.* **178**, 852 (2008).